A computationally efficient superposition T-matrix method for non-spherical particles with overlapping minimum circumscribing spheres

Jesús Rubio
Departamento de Tecnologías de los Computadores y de las Comunicaciones
Universidad de Extremadura
Escuela Politécnica, Avda. de la Universidad, s/n 10003 Cáceres, Spain
E-mail: jesusrubio@unex.es
ORCID: 0000-0002-1424-4714

Rafael Gómez Alcalá
Departamento de Tecnologías de los Computadores y de las Comunicaciones
Universidad de Extremadura
Escuela Politécnica, Avda. de la Universidad, s/n 10003 Cáceres, Spain
E-mail: rgomezal@unex.es
ORCID: 0000-0002-6472-8987

Yolanda Campos-Roca (corresponding author)
Departamento de Tecnologías de los Computadores y de las Comunicaciones
Universidad de Extremadura
Escuela Politécnica, Avda. de la Universidad, s/n 10003 Cáceres, Spain
E-mail: ycampos@unex.es
ORCID: 0000-0003-1161-000X

ABSTRACT: Multiple scattering of particles is calculated with the superposition T-matrix method even if their minimum circumscribing spheres overlap. Starting from the T-matrix of arbitrarily shaped particles, mutual interactions are computed using, exclusively, addition theorems for spherical vector waves. Although a similar idea has been published recently for the two-element case, its extension to an arbitrary number of particles can be very complicated and even unfeasible. In this work, a new, more efficient approach is proposed that provides practically the same results. In addition, it allows its easy application to an arbitrary number of particles simultaneously with the classical superposition T-matrix formulation.

KEYWORDS: Electromagnetic scattering; T-Matrix; spherical vector waves; Addition Theorems

1. Introduction

One of the most powerful methods of particle multiple scattering analysis is based on the calculation of the T-matrix of an isolated element and the translation of spherical vector waves (SVWs) [1]. This method, usually known as the superposition T-matrix method, has been widely utilized for several decades up to the present [2-6]. It has been applied to a great variety of problems such as particle scattering modeling in astronomy, oceanography, photographic science, antennas, meteorology, plasmonic devices, light emitting diodes or solar cells [1,4,5]. The significance of this method has been recently reflected in [7], which proposes a common data format for storing the electromagnetic scattering response using the T-matrix formalism. Most of these works are based on computing this translation by applying addition theorems for SVWs [8-10] between particles whose minimum circumscribing spheres do not overlap, as it is a purely analytical method.

The minimum circumscribing sphere of an object is defined as the sphere with the smallest radius that completely encloses the object. It is commonly used in this context because it requires the smallest degree of SVW expansion to achieve a given level of accuracy. Fig. 1 shows the minimum circumscribing spheres for two particles in two scenarios: one without overlap and one with. The two spheres overlap when the distance between their centers is smaller than the sum of their radii.

[Insert Fig. 1 here]

Classical numerical methods in the field of computational electromagnetics, like the Method of Moments (MoM), are usually much less efficient since they require a much larger number of unknowns per scatterer even for simple structures such as Perfect Electric Conductor (PEC) spheres. In addition, the matrix system is built numerically. In contrast, in the superposition T-matrix method, the system is usually built analytically by using the addition theorems and the number of unknowns is given by the number of SVWs. This number only depends on the electrical size of the scatterer whatever its complexity. For more complex particle geometries, numerical methods such as the Finite Element Method (FEM) and the Finite-Difference in Time-Domain (FDTD) method are usually preferred. However, the size of the equation system increases greatly with the size of the total problem since the volume between particles must also be meshed. In addition, large meshes are difficult to generate and result in poor quality elements that worsen the condition of the matrix system.

It is well known that addition theorems are always valid when the minimum possible sphere circumscribing the scatterer does not overlap with any minimum sphere circumscribing neighboring elements [3]. Although it was established in [11] that this condition could not be necessary due to the analytic continuation of the solution in the entire space, this has only been shown for two scatterers, smaller than half a wavelength. That was possible by greatly increasing the maximum order of the SVWs and computing the T-matrix of the isolated scatterer in quadruple precision. The combined result yielded a huge increase in computational effort. From a purely mathematical point of view, this result can be justified by the fact that, in the case of strongly overlapping minimum spheres, convergence is extremely slow for addition theorems formulas, leading to a high number of coefficients in the expansion. This implies computing very high order Hankel functions in relation to their argument, which provides very high translation matrix coefficients due to the singularity of these functions. Therefore, it will require greater precision in the calculation of T-matrix coefficients to keep the multiple scattering computation precision. A similar explanation was given in [12].

A good way to avoid the limitations of addition theorems in the translation of SVWs is to use an intermediate conversion to plane waves. That is, translation is done by plane waves instead of addition theorems [13]. This idea was presented in [14] reporting excellent results. Although the calculation of translation matrices can be greatly speeded up by using symmetry properties [15], its major drawback is that it needs to solve Sommerfeld integrals carefully and poor convergence problems can arise [16,17].

Another approach that avoids the limitations of the direct application of addition theorems was introduced in [18] and [19] for antenna coupling. That method is based on the use of equivalent infinitesimal dipoles to model the isolated element [20] and the subsequent coupling of such models, exclusively using addition theorems in the whole process. A similar but more elaborated idea has been recently shown in [21], by distributing multipolar sources across the topological skeleton of the scatterer. The major drawback of these procedures is the difficulty to obtain an equivalent model with great precision.

A different method also based exclusively on the use of addition theorems has been proposed in [22] for the case of two scatterers whose minimum spheres overlap. This is achieved by previously translating the origins of the local coordinates of the scatterers using addition theorems, so that the minimum spheres of such scatterers referred to the new centers do not overlap. Subsequently, addition theorems are applied to the T-matrices of each scatterer in its new local coordinate system, to translate the SVWs between them. Then, the T-matrix of the set is expressed in a global coordinate system by translating the origins of the local coordinate systems to this global one. Consequently, the size of the T-matrices in their new coordinate system increases, and therefore also the final matrix system, as the particles are closer together. In addition, this method must be applied iteratively to analyze multiple scattering [3,22]. Unfortunately, it could imply working with enormous T-matrices, and some configurations may even be impossible to analyze, as we will show below.

In this work, it is introduced the use of a different approach, where the translation matrix is computed with the scatterers centered in their original local systems of their minimum spheres. To this aim, consecutive translations of SVWs are evaluated making use of addition theorems to build the translation matrix. In contrast to the methodology suggested in [22], this approach makes it possible to calculate the multiple scattering of an arbitrary number of particles at once, in a simpler and more efficient way. In addition to the series truncation error in the SVW expansion, the proposed method (as well as in works [14-17]) introduces an additional convergence control parameter on the translation matrix coefficients themselves. The result is an approximate translation matrix, which has better convergence behavior but limited final precision. In this way, this approach provides sufficient precision with a much lower degree in the SVW expansion compared to [11], and without needing to increase the order of precision in computing to quadruple precision or higher. Consequently, the cost is greatly reduced with respect to the direct use of translation theorems, as proposed in [11].

Several examples will be shown as a comparison with the results obtained in [22], those obtained by direct calculation as in [11] and with commercial software.

Section 2 presents the theoretical development. Firstly, the superposition T-matrix method is summarized. Next, the implementation method to estimate the translation matrix of SVWs for overlapping minimum spheres is presented. It is based exclusively on addition theorems. And finally, a brief discussion on the number of SVWs is given. In section 3 various cases are presented, each of them with a different purpose. In the first case, the computational cost and applicability of the proposed method is compared with the one discussed in [22]. In the second case, the convergence and accuracy are studied in relation to the method of [22] and to the method based on an intermediate conversion to plane waves [14]. In the third case, the efficiency and the selection of parameters for the proposed method is evaluated. Finally, section 4 is devoted to state the conclusions.

2. Materials and methods

2.1 The superposition T-matrix method

An isolated particle i in a homogeneous medium can be completely described by its T-matrix as

$$\mathbf{T}_i \mathbf{a}_i = \mathbf{b}_i \tag{1}$$

where $\mathbf{a}_i$ and $\mathbf{b}_i$ are column vectors containing, respectively, the complex amplitudes of regular and outgoing spherical vector wave functions (SVWFs) in which the incident and the scattered field for the particle are expanded. These SVWFs are referred to a local coordinate system whose center is the one that defines the minimum sphere circumscribing the particle.

On the other hand, two different particles can be related by a general translation matrix of SVWs, $\mathbf{G}_{ij}$, between them

$$\mathbf{a}_i^{(j)} = \mathbf{G}_{ij}\mathbf{b}_j. \tag{2}$$

In this way, the incoming field in particle *i* coming from particle *j*, which is expanded in regular SVWFs with complex amplitudes $\mathbf{a}_i^{(j)}$, is obtained by translation of the field scattered by particle *j*, which is expanded in outgoing SVWFs with complex amplitudes $\mathbf{b}_j$.

The total incident field on a particle belonging to a group of *N* particles can be expressed as the incident field coming directly from outside the group plus the incident field coming from the rest of particles. Expressing this in terms of complex amplitudes of regular SVWFs and making use of (2) it follows that

$$\mathbf{a}_i = \mathbf{a}_{di} + \sum_{\substack{j=1 \\ j\neq i}}^{N} \mathbf{G}_{ij}\mathbf{b}_j. \tag{3}$$

In (3), $\mathbf{a}_{di}$ are the complex amplitudes of the expansion in regular SVWFs of the incident field coming directly from outside.

From (1) and (3) we obtain

$$\mathbf{b}_i = \mathbf{T}_i\mathbf{a}_{di} + \mathbf{T}_i \sum_{\substack{j=1 \\ j\neq i}}^{N} \mathbf{G}_{ij}\mathbf{b}_j. \tag{4}$$

If we consider (4) for each of the *N* particles belonging to the group, we can obtain the T-matrix for the group $\mathbf{T}_\mathrm{g}$, where the SVWs for each particle are referred to its local coordinate system

$$\mathbf{T}_\mathrm{g} = [\mathbf{I} - \mathbf{TG}]^{-1}\mathbf{T}. \tag{5}$$

In (5), $\mathbf{T}$ is a block-diagonal matrix whose elements are the T-matrices for each single (isolated) particle $\mathbf{T}_i$, and $\mathbf{G}$ is a square matrix whose elements are the general translation matrices $\mathbf{G}_{ij}$ given by (2). Thus, the application of this method requires being able to calculate the submatrices $\mathbf{G}_{ij}$ for an aggregate of arbitrarily shaped particles in arbitrary positions.

2.2 General translation matrix by using addition theorems

In this section we will discuss those cases in which the general translation matrix $\mathbf{G}_{ij}$ can be calculated using, exclusively, the three expressions of the addition theorems for SVWs [13, Eq. 5.24-5.26]:

$$\mathbf{M}_p^{(1)}(\boldsymbol{r} - \boldsymbol{r}_{O'}) = \sum_q G_{pq}^{(1)}(\boldsymbol{r}_O - \boldsymbol{r}_{O'})\, \mathbf{M}_q^{(1)}(\boldsymbol{r} - \boldsymbol{r}_O)\,, \tag{6a}$$

$$\mathbf{M}_p^{(3)}(\boldsymbol{r} - \boldsymbol{r}_{O'}) = \sum_q G_{pq}^{(1)}(\boldsymbol{r}_O - \boldsymbol{r}_{O'})\, \mathbf{M}_q^{(3)}(\boldsymbol{r} - \boldsymbol{r}_O), \qquad |\boldsymbol{r} - \boldsymbol{r}_O| > |\boldsymbol{r}_O - \boldsymbol{r}_{O'}| \tag{6b}$$

$$\mathbf{M}_p^{(3)}(\boldsymbol{r} - \boldsymbol{r}_{O'}) = \sum_q G_{pq}(\boldsymbol{r}_O - \boldsymbol{r}_{O'})\, \mathbf{M}_q^{(1)}(\boldsymbol{r} - \boldsymbol{r}_O)\,, \qquad |\boldsymbol{r} - \boldsymbol{r}_O| < |\boldsymbol{r}_O - \boldsymbol{r}_{O'}| \tag{6c}$$

where $\mathbf{M}_p^{(1)}(\boldsymbol{r} - \boldsymbol{r}_O)$ are the regular SVWFs centered in $\boldsymbol{r}_O$ and $\mathbf{M}_p^{(3)}(\boldsymbol{r} - \boldsymbol{r}_O)$ are the outgoing SVWFs. The summation indices *p* and *q* subsume the degree *n*, the order, and the polarization of the SVWs. Coefficients $G_{pq}^{(1)}(\boldsymbol{r}_O - \boldsymbol{r}_{O'})$ and $G_{pq}(\boldsymbol{r}_O - \boldsymbol{r}_{O'})$ will be computed here using a rotation-axial translation-inverse rotation technique [10] [23], although they can be computed using expressions involving the Wigner-3j symbols [13].

The general translation matrix can be then obtained as follows:
1) Calculate the minimum circumscribing spheres for two particles. If their minimum spheres do not overlap, condition in (6c) is always satisfied and the divergence problem of the SVW expansion inside the minimum spheres of arbitrary particles [24] is avoided. Thus, the scattered electric field by particle *j*, $\boldsymbol{E}_{sj}$, expanded in terms of outgoing SVWFs in the local coordinate system of particle *j* centered in *Oj*, the center of its minimum sphere,

$$\boldsymbol{E}_{sj}(\boldsymbol{r}-\boldsymbol{r}_{Oj}) = \sum_{pj} b_{pj}\, \mathbf{M}_{pj}^{(3)}(\boldsymbol{r}-\boldsymbol{r}_{Oj}), \tag{7a}$$

can be translated to the local coordinate center of the minimum sphere of particle *i*, *Oi*, by using (6c)

$$\boldsymbol{E}_{sj}(\boldsymbol{r}-\boldsymbol{r}_{Oi}) = \sum_{pj} b_{pj} \sum_{pi} G_{pj\,pi}(\boldsymbol{r}_{Oi}-\boldsymbol{r}_{Oj})\, \mathbf{M}_{pi}^{(1)}(\boldsymbol{r}-\boldsymbol{r}_{Oi}) \tag{7b}$$

This field will be the incoming electric field in particle *i* coming from particle *j*, $\boldsymbol{E}_i^{(j)}$, expanded in terms of regular SVWFs centered in *Oi*

$$\boldsymbol{E}_i^{(j)}(\boldsymbol{r}-\boldsymbol{r}_{Oi}) = \sum_{pi} a_{pi}^{(j)}\, \mathbf{M}_{pi}^{(1)}(\boldsymbol{r}-\boldsymbol{r}_{Oi}). \tag{7c}$$

By identifying (7b) with (7c), (2) is easily derived, where $G_{pj\,pi}(\boldsymbol{r}_{Oi}-\boldsymbol{r}_{Oj})$ will be the coefficients of the transpose of the general translation matrix $\mathbf{G}_{ij}$. This matrix has been obtained by truncating the SVW expansions in both centers.

2) If their minimum circumscribing spheres overlap, find a plane that separates the two particles, and does not intersect them. If it is not possible to find a separation plane, this methodology is not applicable. Fig. 2 shows two particles *i* and *j* centered in *Oi* and *Oj* respectively, with overlapping minimum circumscribing spheres. A separating plane has been defined between them. They have been placed at the same *y* coordinate in a global coordinate system to simplify the drawing, without loss of generality.

[Insert Fig. 2 here]

3) For each of the two particles, find a new coordinate system so that their new minimum spheres referred to the center of these new coordinate systems do not intersect, i.e., they are, at most, tangent to the separating plane found in step 2). It is important to note that there does not exist a general method that provides a new minimum sphere that is tangent to the separation plane, because it depends on the shape and attitude of the particle. Some cases of interest, where the problem can be reduced to 2D, can be optimally solved using the methods developed for solving one case of the Apollonius' problem. This involves finding the circumference tangent to a line that passes through two points. In any case, a general method can be used that consists of the following procedure. First, find the line l_j perpendicular to the plane that passes through *Oj*. In this line we will locate the new center *Ou*. The position of the new center will be determined by imposing that the distance to the plane is the same as the distance to an extreme point of the particle *E* that is the closest to the plane. In this way, the minimum sphere centered in *Ou* should not intersect either the separating plane or the particle. The same procedure is also applied to the other particle *i*, and a new center *Ov* is then found. Fig 2 shows a 2D representation.

4) Starting from the field scattered by particle *j* given in terms of outgoing SVWFs with complex amplitudes $\mathbf{b}_j$ in its original center *Oj*, given by (7a), translate it to the new center *Ou*

obtained in step 3) by using (6b):

$$\boldsymbol{E}_{sj}(\boldsymbol{r}-\boldsymbol{r}_{Ou}) = \sum_{pj} b_{pj} \sum_{pu} G^{(1)}_{pj\,pu}(\boldsymbol{r}_{Ou}-\boldsymbol{r}_{Oj})\, \mathbf{M}^{(3)}_{pu}(\boldsymbol{r}-\boldsymbol{r}_{Ou}). \tag{8a}$$

This field can be directly expressed in terms of regular SVWFs with complex amplitudes $\mathbf{b}_u$

$$\boldsymbol{E}_{sj}(\boldsymbol{r}-\boldsymbol{r}_{Ou}) = \sum_{pu} b_{pu}\, \mathbf{M}^{(3)}_{pu}(\boldsymbol{r}-\boldsymbol{r}_{Ou}). \tag{8b}$$

By identifying (8a) with (8b), the following matrix expression can be found if the SVW expansions in both centers are truncated

$$\mathbf{b}_u = \mathbf{G}_{\mathbf{1}uj}\mathbf{b}_j, \tag{9}$$

where $G^{(1)}_{pj\,pu}(\boldsymbol{r}_{Ou}-\boldsymbol{r}_{Oj})$ will be the coefficients of the transpose of the decentering matrix $\mathbf{G}_{\mathbf{1}uj}$. The new expansion will converge outside the minimum sphere of the particle at its new center *Ou*, which always satisfies the condition given in (6b). In this way, this procedure changes the convergence region of the expansion in outgoing SVWFs to that provided by the new minimum sphere given by $R_{Ou} > R_{Oumin}$, with R_{Oumin} being the radius of the minimum sphere that circumscribes the particle *j* centered in *Ou* (see Fig. 2). The decentering matrix $\mathbf{G}_{\mathbf{1}uj}$ can be calculated by using rotations and axial translation as follows:

$$\mathbf{G}_{\mathbf{1}uj} = \left[\mathbf{R}_j(\varphi_j)\mathbf{D}_j(\theta_j)\mathbf{C}_{\mathbf{1}}\left(-\left|\boldsymbol{r}_{Ou}-\boldsymbol{r}_{Oj}\right|/\lambda\right)\right]^T. \tag{10}$$

Matrices $\mathbf{R}_j(\varphi_j)$ and $\mathbf{D}_j(\theta_j)$ make it possible the reorientation of outgoing SVWFs for particle *j*. By rotating φ_j and θ_j the original coordinate system of particle *j*, it will have its *x*-*z* plane orthogonal to the separating plane with the *z*-axis orthogonal and oriented towards the plane. $\mathbf{C}_{\mathbf{1}}\left(-\left|\boldsymbol{r}_{Ou}-\boldsymbol{r}_{Oj}\right|/\lambda\right)$ is a matrix that allows for an axial translation of SVWFs from the rotated coordinate system of particle *j* to the new center *Ou*. Elements of these matrices have been defined in [23] and [10]. However, elements of $\mathbf{C}_{\mathbf{1}}\left(-\left|\boldsymbol{r}_{Ou}-\boldsymbol{r}_{Oj}\right|/\lambda\right)$ are computed by using Bessel functions according to the second case of addition theorems for axial translations given in Appendix 3 of [10].

5) Starting from the field scattered by the particle *j* towards particle *i*, given by (8b) in terms of outgoing SVWFs with complex amplitudes $\mathbf{b}_u$ in the new center *Ou*, translate this field to the new center in particle *i*, *Ov,* by using (6c)

$$\boldsymbol{E}_{sj}(\boldsymbol{r}-\boldsymbol{r}_{Ov}) = \sum_{pu} b_{pu} \sum_{pv} G_{pu\,pv}(\boldsymbol{r}_{Ov}-\boldsymbol{r}_{Ou})\, \mathbf{M}^{(1)}_{pv}(\boldsymbol{r}-\boldsymbol{r}_{Ov}) \tag{11a}$$

This field will be the incoming field in particle *i* coming from particle *j*, expressed in terms of regular SVWFs with complex amplitudes $\mathbf{a}^{(j)}_v$ referred to the new center in particle *i*, *Ov*

$$\boldsymbol{E}^{(j)}_i(\boldsymbol{r}-\boldsymbol{r}_{Ov}) = \sum_{pv} a^{(j)}_{pv}\, \mathbf{M}^{(1)}_{pv}(\boldsymbol{r}-\boldsymbol{r}_{Ov}). \tag{11b}$$

It should be noted that condition in (6c) is now satisfied. The divergence problem of the SVW expansion inside the minimum circumscribing spheres of arbitrary particles [24] is avoided since minimum spheres of particles referred to the new centers *Ou* and *Ov* do not overlap (see Fig. 2). By identifying (11a) with (11b), the usual expression for non-overlapping minimum spheres in matrix form is obtained when the SVW expansions in the new centers are truncated:

$$\mathbf{a}_v^{(j)} = \mathbf{G}_{vu}\mathbf{b}_u. \tag{12}$$

where $G_{pu\,pv}(\boldsymbol{r}_{Ov} - \boldsymbol{r}_{Ou})$ will be the coefficients of the transpose of the general translation matrix $\mathbf{G}_{vu}$.

By using addition theorems for axial translation and rotation properties [10][23] we have

$$\mathbf{G}_{vu} = [\mathbf{R}_u(\varphi_u)\mathbf{D}_u(\theta_u)\mathbf{C}(|\boldsymbol{r}_{Ov} - \boldsymbol{r}_{Ou}|/\lambda)\ \mathbf{D}_v(\theta_v)\mathbf{R}_v(\varphi_v)]^T. \tag{13}$$

In (9), φ_u and θ_u orientate the *z*-axis in the coordinate system associated to center *Ou* towards center *Ov*, by a φ-rotation followed by a θ-rotation. Matrices $\mathbf{R}_u(\varphi_u)$ and $\mathbf{D}_u(\theta_u)$ perform these rotations for the outgoing SVWFs referred to center *Ou*. $\mathbf{C}(|\boldsymbol{r}_{Ov} - \boldsymbol{r}_{Ou}|/\lambda)$ is a matrix that allows for an axial translation of the coordinate system from center *Ou* to center *Ov*, relating outgoing to regular SVWFs. Finally, θ_v and φ_v orientate the *z*-axis associated to center *Ov* orthogonal to the separating plane. It can be achieved by a θ-rotation followed by a φ-rotation of the regular SVWFs referred to center *Ov*, by using matrices $\mathbf{D}_v(\theta_v)$ and $\mathbf{R}_v(\varphi_v)$, respectively.

6) Starting from the incident field in particle *i* coming from particle *j*, given in terms of regular SVWFs referred to center *Ov* (11b), translate this field to the original coordinate system of particle *i*, centered in *Oi*, by making use of (6a)

$$\boldsymbol{E}_i^{(j)}(\boldsymbol{r} - \boldsymbol{r}_{Oi}) = \sum_{pv} a_{pv}^{(j)} \sum_{pi} G_{pv\,pi}^{(1)}(\boldsymbol{r}_{Oi} - \boldsymbol{r}_{Ov})\ \mathbf{M}_{pi}^{(1)}(\boldsymbol{r} - \boldsymbol{r}_{Oi}). \tag{14a}$$

This field in the same coordinate system can be directly expressed in terms of regular SVWFs with complex amplitudes $\mathbf{a}_i^{(j)}$

$$\boldsymbol{E}_i^{(j)}(\boldsymbol{r} - \boldsymbol{r}_{Oi}) = \sum_{pi} a_{pi}^{(j)}\ \mathbf{M}_{pi}^{(1)}(\boldsymbol{r} - \boldsymbol{r}_{Oi}) \tag{14b}$$

From (14a) and (14b) the following matrix expression is found if the SVW expansion in both centers *Ov* and *Oi* is truncated

$$\mathbf{a}_i^{(j)} = \mathbf{G}_{\mathbf{1}iv}\ \mathbf{a}_v^{(j)}\ , \tag{15}$$

where $G_{pv\,pi}^{(1)}(\boldsymbol{r}_{Oi} - \boldsymbol{r}_{Ov})$ will be the coefficients of the decentering matrix $\mathbf{G}_{\mathbf{1}iv}$. This matrix can be calculated by using rotations and axial translation as

$$\mathbf{G}_{\mathbf{1}iv} = [\mathbf{C}_{\mathbf{1}}(-|\boldsymbol{r}_{Oi} - \boldsymbol{r}_{Ov}|/\lambda)\mathbf{D}_i(\theta_i)\mathbf{R}_i(\varphi_i)]^T. \tag{16}$$

In (16), $\mathbf{C}_{\mathbf{1}}(-|\boldsymbol{r}_{Oi} - \boldsymbol{r}_{Ov}|/\lambda)$ is a matrix that allows for an axial translation of SVWs from center *Ov* to the original center *Oi* of particle *i*. Matrices $\mathbf{D}_i(\theta_i)$ and $\mathbf{R}_i(\varphi_i)$ make it possible the reorientation of the regular SVWFs of particle *i* after recentering. By rotating θ_i and φ_i, the local coordinate system will coincide with the original local coordinate system of particle *i* centered in *Oi*.

7) Calculate the general translation matrix given by (2) from (9), (12) and (15)

$$\mathbf{G}_{ij} = \mathbf{G}_{\mathbf{1}iv}\ \mathbf{G}_{vu}\mathbf{G}_{\mathbf{1}uj}\ . \tag{17}$$

In the particular case of having a separating plane orthogonal to the direction of the line joining the original centers of particles *i* and *j*, $\mathbf{G}_{vu}$ reduces to

$$\mathbf{G}_{vu} = [\mathbf{C}(|\boldsymbol{r}_{Ov} - \boldsymbol{r}_{Ou}|/\lambda)]^T. \tag{18}$$

It should be noted that the equality given by (17) is true only if infinite terms are retained in the SVW expansions in the new coordinate systems obtained in step 3). Since these SVW expansions must be truncated, the general translation matrix thus obtained is an approximation to the exact general translation matrix, but with an extra convergence control parameter given by the maximum degree of these intermediate expansions. Truncation of the SVW expansions results in the highest value coefficients of the general translation matrix $\mathbf{G}_{ij}$ being truncated. These coefficients arise from the evaluation of high-order Hankel functions. They are responsible for the divergence of the solution as we are working with a finite precision to compute the T-matrix. Excessive truncation of these coefficients provides results with lower precision, but insufficient truncation of them still produces a wrong result. Increasing the accuracy of the T-matrix by adding coefficients related to higher order SVWs will permit a smaller truncation of the highest coefficients of the general translation matrix. In this way, the result will converge in a greater margin of values of maximum degree of the intermediate expansion. This will in principle improve the precision, although this improvement may become very insignificant in those cases in which the precision of the T-matrix is good enough for the distance between particles studied.

Therefore, we will have a relative convergence problem that will need to be studied. As shown in section 3, results that converge better towards the solution can be found by means of an adequate selection of these maximum degrees, at the cost of providing a limited maximum precision.

2.3 Number of SVWs

In order to compute (17), the maximum degree values of the SVW expansion in its original coordinate system (n_{jmax}) and in the coordinate system associated to the new center ($n_{\mathrm{d}jmax}$) should be chosen for each particle.

As explained in [15], n_{jmax} should be chosen to provide the desired accuracy. The criterion given in [25] can be applied:

$$n_{jmax} = \left[kr_{Omin} + 0.045\sqrt[3]{kr_{Omin}}\,(-Ptr\,)\right], \tag{19}$$

where r_{Omin} is the radius of the minimum circumscribing sphere in the original coordinate system, k is the wavenumber and Ptr is the relative truncated (i.e., excluded due to the series truncation) power in dB with respect to the total radiated power. Because of the very close interactions in case of overlapping minimum spheres, it was verified in [14] that very good results are obtained by choosing Ptr equal to -130 dB for elements with a minimum sphere with radius less than a half wavelength. However, in the case of elements referred to a center far away from them, we have observed that (19), choosing Ptr equal to -130 dB, cannot be enough to estimate $n_{\mathrm{d}jmax}$. Therefore, convergence studies will be presented in the next section.

3. Results and discussion

3.1 Computational cost and applicability

The computational cost and applicability of the method is compared with the one presented in [22]. For this purpose, we first study two PEC disks, infinitely thin, with radii equal to a wavelength. Unlike [22], which uses an analytical method to obtain the T-matrix of a single (isolated) disk, here it will be computed with the FEM [26]. In future work, it would be more convenient to use, whenever possible, T matrices that have already been computed by other researchers [7]. However, for particles with arbitrary shapes and compositions, for which such precomputed data may not be available, the FEM [26] can still be applied.

In [22], the chosen maximum index n_{jmax} was 20 for the T-matrix of the single disk in its original center (the disk center). From this T-matrix, two T-matrices referred to new centers so that their minimum circumscribing spheres do not overlap were obtained in that work. The maximum index for both T-matrices in the new centers (equivalent to n_{djmax}) was found through a convergence study, being 32 for a separation distance of half a wavelength. With the resulting T-matrices, the total two-disk T-matrix was computed using an expression given in [3] for two scatterers. This expression requires the inversion of two matrices with a size equal to the resulting T-matrices. Thus, the larger the overlap, the larger the size of the matrices to be inverted in [22]. However, with the approximation proposed in this work, the size of the matrices to invert is always the same, whatever the distance between the particles. It has been also reported the same example but with a smaller separation between the disks (larger overlapping), equal to 0.2 wavelengths. Table 1 shows the size of the matrices to be inverted in [22] in contrast with the size needed in this work when the same expression is used to compute the total T-matrix.

Fig. 3 shows the normalized bistatic radar cross section (RCS) of the two PEC disks separated by half a wavelength. It has been obtained for a 60º incident angle, compared with the results in [22] and a FEM simulation of the whole structure using the method provided in [26]. To obtain these results we have applied the same parameters as in [22], i.e., n_{jmax} was 20 and $n_{\mathrm{d}jmax}$ was 32. It can be observed that the three results are practically identical.

[Insert Table 1 here]

[Insert Fig. 3 here]

The scattering of more than two particles can be easily dealt with by (5). However, in [22] the author does not solve any problem of more than two scatterers. The method suggested in [22] for more than two scatterers is based on forming a multi-scatterer in an iterative process to build a new multi-scatterer T-matrix. Unfortunately, this strategy can be very inefficient as the number of scatterers increases. In this sense, the example drawn in Fig. 4 is illustrative, where only eight scatterers have been drawn. To consider a higher number, additional scatterers are added forming two rows of parallel disks with radii equal to a wavelength separated 0.5 wavelengths. In turn, the top row is horizontally displaced by a distance equal to one wavelength with respect to the bottom row. In this way, the minimum spheres of contiguous scatterers overlap each other as shown in Fig. 4. For this example, a good strategy to apply the method suggested in [22] is to group the disks two by two and group the result with another group of four, and so on.

[Insert Fig. 4 here]

Fig. 5 compares the sizes of the matrices to be inverted for both methods. In the method of

[22], only the size of the matrices in the last iteration is shown. In order to compute $n_{\mathrm{d}jmax}$ for each group of scatterers, the value provided by (19) choosing Ptr equal to -130 dB has been used. This underestimates the real value needed to achieve convergence in cases of highly decentered spheres, as it will be shown later. Therefore, for our approach we really show the total effort whereas for the method in [22] the effort is always greater than the effort shown in the figure. Even so, it can be seen that our method requires much less effort than this one as the number of scatterers increases. It should also be observed that, when grouping scatterers, the degree of the SVWs increases rapidly. Thus, in this example, for a group of only 8 scatterers a value of $n_{\mathrm{d}jmax}$ equal to 700 is needed. This makes computing the decentering and coupling matrices of SVWs much more costly.

[Insert Fig. 5 here]

3.2 Convergence and accuracy

Two PEC spheroids are considered in this subsection. They have a major axis b of 0.6λ and a minor axis a of 0.25b. Separation between original centers is equal to 0.3λ (0.15λ between the edges of the spheroids), as shown in Fig. 6a.

It is first solved by using a 0.78λ separation between the new centers to compute (17), which is slightly higher than the minimum distance needed to avoid the overlapping problem in the computation.

Fig. 7 shows the convergence of our result, compared with the FEM result of the whole structure. The accuracy is computed as an approximate number of decimal digits in the computation of T-matrix for the whole structure as a function of the maximum degree values of the SVW expansion in the coordinate system associated to the new center (n_{djmax}), chosen to compute (17). It is given as a family of curves for different values of the maximum degree of the SVW expansion in its original coordinate system (n_{jmax}). The approximate number of decimal digits is given by -log(RE) [27], where RE is the relative error defined as:

$$\mathrm{RE} = \frac{\|\mathbf{T}_{\mathrm{a}} - \mathbf{T}_{\mathrm{FEM}}\|}{\|\mathbf{T}_{\mathrm{FEM}}\|} \tag{20}$$

$\mathbf{T}_{\mathrm{a}}$ is the T-matrix computed with the proposed method, but with all the SVWs referred to the same coordinate system, and $\mathbf{T}_{\mathrm{FEM}}$ is the T-matrix computed with FEM, that is taken as a reference solution.

[Insert Fig. 6 here]

If (19), choosing Ptr equal to -130 dB, were used directly instead of doing a convergence study, this would give good results in this case. Thus, an n_{jmax} value of 9 and an $n_{\mathrm{d}jmax}$ value of 10 are obtained, which provide a 3.68 digits accuracy according to Fig. 7.

The same example is next solved by increasing the distance between new centers to 1.5λ to compute (17). Fig 8 shows the convergence of our result, compared with the FEM result. It is worth noting that increasing the distance between new centers does not improve the precision of the results. However, the computational effort to compute (17) is strongly increased since an $n_{\mathrm{d}jmax}$ of 18 is needed to obtain the same accuracy. The value provided by (19) was 14 with a Ptr of -130 dB, and therefore, according to Fig. 8, it does not provide such a good estimation in this case.

These new centers were also considered to solve the same problem with the method provided in [22]. The obtained accuracy practically coincides with that shown in Fig. 8, with a maximum difference in the RE of 10^{-5} between both methods. Therefore, both methods provide the same results. However, the method described in [22] requires the inversion of two matrices with a size of 720 (2×18×20). In contrast, the computational effort of our method implies the inversion of two matrices with a size of 198 (2×9×11).

[Insert Fig. 7 here]

[Insert Fig. 8 here]

It should be noted that these new centers allow reducing the distance between spheroids edges to 0.0375λ, where a very strong overlapping occurs (see Fig. 6b). Fig. 9 shows the convergence in this case, where the behavior is similar to the one shown in Fig. 8, but the maximum accuracy is approximately half, due to the close proximity between the spheroids. Fig. 10 presents the monostatic RCS results for the two-spheroid cases depicted in Figs. 6a and 6b. It can be observed that the result for 6b is slightly shifted compared to that obtained with FEM, because the approximate number of decimal digits is lower in this case, which is consistent with the results shown in Figs. 7 and 9.

[Insert Fig. 9 here]

[Insert Fig. 10 here]

The application of the proposed method provides the same convergence pattern for every case of study. That is, for a starting accuracy given by the degree of expansion in SVWs used to obtain the T-matrix of isolated particles (n_{jmax}), the accuracy of the results increases progressively as the degree of the SVWs in the new center (n_{djmax}) until it sharply drops. The range of n_{djmax} values where the problem has converged is wider the greater the initial precision and the longer the decentering distance. However, choosing a longer decentering distance increases the value of n_{djmax} required to obtain the same accuracy and, consequently, the computational effort. This is a well-known behavior of relative convergence, which also occurs in the method used in [14] and [15] and which has been well documented in [17]. Fig. 11 shows the convergence of the result obtained for the case depicted in Fig. 6a, by using a transformation to plane vector waves to compute the translation matrix [14]. It is clearly noticed that these results present almost the same maximum accuracy than the results shown in Figs. 7 and 8 for the proposed method and the same convergence behavior.

[Insert Fig. 11 here]

Fig. 12 shows the magnitude of the non-zero coefficients of three columns of general translation matrices. Three matrices are compared: the translation matrix computed using the proposed method to obtain the results in Fig. 8 with $n_{djmax} = 22$, the translation matrix computed using the method based on transformation to plane waves to obtain the results in Fig. 11 with $\bar{\kappa}_{tr} = 3.75$ for similar accuracy, and that obtained with the direct method that computes it as in the non-overlapping case. Both the proposed method and the one based on plane wave transformation, truncate the highest coefficients in a similar way in relation to the direct method. It can also be observed that the truncation is greater as the degree of the SVW expansion (n_{jmax}) increases. This value has been represented on the abscissa axis. These results are in agreement with the reasoning given in section 2.2.

[Insert Fig. 12 here]

3.3 Efficiency and selection of the truncation degree

Although the number of SVWs needed in the T-matrix of the isolated element is greater in the case of overlapping of minimum spheres, the proposed method is still more efficient than classical numerical methods in computational electromagnetics.

Fig. 13 shows the computing time required to calculate the monostatic RCS for the case given in Fig. 6a as a function of the number of spheroids placed in parallel. Results are given for different numbers of incidence directions. It compares the computing times obtained using the commercial software CST [28] and the presented method. The commercial software uses the optimal solver method for the MoM in each case (a direct solver, for 11 spheroids, and Multilevel Fast Multipole Method (MLFMM), in the rest of the cases) whereas we use a conventional direct solver. As can be seen, our method is much faster in all cases, even for such a simple scatterer. More complex geometries will lead to much larger computing time differences between both methods. Fig. 14 shows the monostatic RCS for a case with 11 spheroids. An excellent agreement with commercial software can be observed since they present a match of practically three significant digits. It is also provided the array factor response, which is obtained without considering the mutual interactions, to note their effect between the spheroids. It is computed by making $\mathbf{G} = \mathbf{0}$ in (5).

[Insert Fig. 13 here]

[Insert Fig. 14 here]

Fig. 15 shows the results for the same case, obtained by applying the direct method that computes the translation matrix as in the non-overlapping case, compared with the results obtained in this work for different values of n_{jmax}. We have used $n_{\mathrm{d}jmax} = 9$, with n_{jmax} between 5 and 9 for the proposed method with a distance of 0.78λ between the new centers of close spheroids with overlapping minimum spheres. They have been chosen according to the two-spheroid case studied in Fig. 7, which ensures more than two digits of precision, and are directly used for different sizes of particle groups. The results obtained with the proposed method are indistinguishable since the maximum deviation found between them is 0.5%, which corresponds to two hundredths of a decibel at the worst angle. However, none of these values of n_{jmax} provides an accurate result using the direct method. In all the cases, double precision has been used in the computation with Matlab. For n_{jmax}=9 in the direct computation, the matrix to invert in (5) is close to singular (rcond=1.03E-17).

Figure 16 shows the results obtained by setting $n_{jmax} = 5$, with n_{djmax} from 9 to 14. The result obtained is in accordance with Fig. 7, where the accuracy decreases as n_{djmax} increases. It can be seen that, for a precision of less than 1.5 digits the results begin to move away from the correct result obtained with $n_{djmax} = 9$. Therefore, results in Figs. 15 and 16 confirm that the convergence study for two spheroids can be used for the study of an aggregate of an arbitrary number of the same spheroids.

The convergence study for two particles could be avoided if a formula were available that provided the optimum value of parameter n_{djmax} as a function of the decentered radius and n_{jmax}. In this sense, in order to estimate the optimum $n_{\mathrm{d}jmax}$, several cases of two spheroids have been studied for a typical size of particles with a minimum-sphere radius up to 0.45λ and n_{jmax} equal to 10. It has been found the following phenomenological formula

$$n_{\mathrm{d}jmax} = \left[7.58\left(\frac{r_{Odmin}}{r_{Omin}} - 1\right) + 10\right] \tag{21}$$

where $r_{Omin}$and r_{Odmin} are the radius of the minimum sphere in the original center and in the new center respectively, and [ ] denotes the closest integer value. This formula is built from the baseline case consisting of non-overlapping spheres. In that case, decentering is not required and thus we can consider $r_{Odmin} = r_{Omin}$. It should be noted that for a r_{Omin} lower than approximately 0.37λ, very good results can be obtained with lower values of n_{jmax}. However, for such values (21) is no longer applicable since it has been obtained fixing $n_{jmax} = 10$. The different cases considered to calculate the slope in (21) are generated by considering variations in the spheroid dimensions (minor axis) and different values for the separation between original centers. This variety of parameter values led to different r_{Odmin}/r_{Omin} ratios, and for each case $n_{\mathrm{d}jmax}$ was obtained. It was observed that the relationship between $n_{\mathrm{d}jmax}$ and r_{Odmin}/r_{Omin} followed an approximately linear pattern, so finally the slope was estimated by applying linear regression on the calculated $n_{\mathrm{d}jmax}$ values. This formula has been successfully applied to such complicated objects as arrays of patch or dielectric resonator antennas located in close proximity. These results will not be shown here for the sake of brevity.

[Insert Fig. 15 here]

[Insert Fig. 16 here]

4. Conclusion

In this work it has been shown that the classical formulation of the superposition T-matrix method can be utilized even if the minimum circumscribing spheres for the particles overlap. To this aim, a new approach has been introduced. It is based on approximating the general translation matrix as a product of three matrices. These matrices are computed by using addition theorems and rotation properties. They represent decentering, translation and recentering operations, respectively. This approach is more efficient and systematic than a previously one found in the literature, which is based on the previous computation of decentered T-matrices, giving practically the same accuracy for the two-element case.

The article presents the formal computational framework of the proposed method, accompanied by an initial collection of case studies that highlight its advantages. Future research on the methodology should involve additional case studies to further explore its characteristics, for example, aiming to derive more general equations that ensure convergence without the need of previous studies. The method gives researchers the ability to expand the range of applicability of their superposition T-matrix codes with a small effort. Within this widening, the method is applicable in a great variety of problems, practically eliminating the restriction of separation distance between elements, such as: sensing of atmospheric particles, the performance of astrophysical studies, analysis and design of antenna arrays, computing RCS for military applications, optimization of light scattering for plasmonic devices, light-emitting diodes, or solar cells.

Funding. This work was supported by MICIU/AEI/ 10.13039/501100011033 (Agencia Estatal de Investigación, Spain) and by ERDF A Way of making Europe (European Union), under Grant PID2021-122856NB-C21.

Disclosure statement. The authors declare no conflicts of interest.

References

1. M. I. Mishchenko, G. Videen, V. A. Babenko, N. G. Khlebtsov, and T. Wriedt, "T-matrix theory of electromagnetic scattering by particles and its applications: a comprehensive reference database," J. Quant. Spectrosc. Radiat. Transfer 88(1–3), 357–406 (2004), https://doi.org/10.1016/j.jqsrt.2004.05.002.

2. J. H. Bruning and Y. T. Lo, "Multiple scattering of EM waves by spheres, part I—Multipole expansion and ray-optical solutions and Part II—Numerical and experimental results," IEEE Trans. Antennas Propag. **19**, 378–400 (1971), https://doi.org/10.1109/TAP.1971.1139925.
3. B. Peterson and S. Ström, "T-matrix for electromagnetic scattering from an arbitrary number of scatterers and representations of E(3)," Phys. Rev. D 8, 3661–78 (1973), https://doi.org/10.1103/PhysRevD.8.3661.
4. M. I. Mishchenko, N. G. Khlebtsov, G. Videen, T. Wriedt, and N. T. Zakharova, "Comprehensive T-matrix reference database: a 2015–17 update," J. Quant. Spectrosc. Radiat. Transfer 202, 240–6 (2017), https://doi.org/10.1016/j.jqsrt.2017.08.007.
5. M. I. Mishchenko, "Comprehensive thematic T-matrix reference database: a 2017–2019 update," J. Quant. Spectrosc. Radiat. Transfer 242, 1–9 (2020), https://doi.org/10.1016/j.jqsrt.2019.106692.
6. Y. C. Tzeng, and A. K. Fung, "T-matrix approach to multiple scattering of EM waves from N-spheres, " Journal of Electromagnetic Waves and Applications, 8(1), 61–84 (1994), https://doi.org/10.1163/156939394X00812.
7. N. Asadova, K. Achouri, K. Arjas, B. Auguié, R. Aydin, A. Baron, et al., "T-matrix representation of optical scattering response: Suggestion for a data format," J. Quant. Spectrosc. Radiat. Transfer 333, 109310 (2025), https://doi.org/10.1016/j.jqsrt.2024.109310.
8. S. Stein, "Addition theorem for spherical wave functions," Q. Appl. Math. **19**, 15–24 (1961).
9. O. R. Cruzan, "Translational addition theorem for spherical vector wave functions," Q. Appl. Math. **20**, 33–40 (1962).
10. J. E. Hansen (Ed.), *Spherical Near-Field Antenna Measurements* (London, U.K.: Peter Peregrinus Ltd.,1988).
11. D. Schebarchov, E. C. Le Ru, J. Grand, and B. Auguié, "Mind the gap: testing the Rayleigh hypothesis in T-matrix calculations with adjacent spheroids," Opt. Express 27, 35750-35760 (2019), https://doi.org/10.1364/OE.27.035750.
12. A. Doicu, Y. A. Eremin, and T. Wriedt, "Convergence of the T-matrix method for light scattering from a particle on or near a surface," Opt. Commun. 159, 266-277 (1999), https://doi.org/10.1016/S0030-4018(98)00586-0.
13. A. Boström, G. Kristensson, and S. Ström. "Transformation properties of plane, spherical and cylindrical scalar and vector wave functions," in Field Representations and Introduction to Scattering (Elsevier Science Publishers, 1991). Ch. 4:165-210.
14. D. Theobald, A. Egel, G. Gomard, and U. Lemmer, "Plane-wave coupling formalism for T-matrix simulations of light scattering by nonspherical particles," Phys. Rev. A **96**, 1-8 (2017). doi: 10.1103/PhysRevA.96.033822.
15. J. Rubio and R. Gómez-Alcalá, "Mutual coupling of antennas with overlapping minimum spheres based on the transformation between spherical and plane vector waves," IEEE Trans. Antennas Propag. 69(4), 2103-2111 (2021), https://doi.org/10.1109/TAP.2020.3026882.
16. A. Egel, D. Theobald, U. Lemmer, and G. Gomard, "Light scattering by oblate particles near planar interfaces: on the validity of the T-matrix approach," Opt. Express 24(22), 25154 (2016), https://doi.org/10.1364/OE.24.025154.
17. A. Egel, Y. Eremin, T. Wriedt, D. Theobald, and G. Gomard, "Extending the applicability of the T-matrix method to light scattering by flat particles on a substrate via truncation of Sommerfeld integrals," J. Quant. Spectrosc. Radiat. Transfer 202, 279–285 (2017), https://doi.org/10.1016/j.jqsrt.2017.08.016.
18. J. F. Izquierdo, J. Rubio, and J. Zapata, "Antenna-generalized scattering matrix in terms of equivalent infinitesimal dipoles: Application to finite array problems," IEEE Trans. Antennas Propag. 60(10), 4601–4609 (2012), https://doi.org/10.1109/TAP.2012.2207348.
19. J. F. Izquierdo, J. Rubio, and J. Zapata, "Spherical-waves-based analysis of arrays of volumetric antennas with overlapping minimum spheres," IEEE Antennas Wirel. Propag. Lett. 11, 1296-1299 (2012), https://doi.org/10.1109/LAWP.2012.2227234.
20. Y. Adane, A. Gati, M. F. Wong, C. Dale, J. Wiart, and V. F. Hanna, "Optimal modeling of real radio base station antennas for human exposure assessment using spherical-mode decomposition," IEEE Antennas Wirel. Propag. Lett. 1, 215–218 (2002), https://doi.org/10.1109/LAWP.2002.807960.
21. A. G. Lamprianidis, C. Rockstuhl, and I. Fernandez-Corbaton, "Transcending the Rayleigh Hypothesis with multipolar sources distributed across the topological skeleton of a scatterer," J. Quant. Spectrosc. Radiat. Transfer 296, 108455 (2023), https://doi.org/10.1016/j.jqsrt.2022.108455.
22. T. Martin, "T-matrix method for closely adjacent obstacles," J. Quant. Spectrosc. Radiat. Transfer 234, 40–46 (2019), https://doi.org/10.1016/j.jqsrt.2019.06.001.
23. J. Rubio, M.A. González, and J. Zapata, "Generalized-scattering-matrix analysis of a class of finite arrays of coupled antennas by using 3-D FEM and spherical mode expansion," IEEE Trans. Antennas Propag. 53(3), 1133–1144 (2005), https://doi.org/10.1109/TAP.2004.842687.
24. B. Auguié, W. R. C. Somerville, S. Roache, E. C. Le Ru, "Numerical investigation of the Rayleigh hypothesis for electromagnetic scattering by a particle," J Opt, 18, 075007 (2016), https://doi.org/10.1088/2040-8978/18/7/075007.
25. F. Jensen and A. Frandsen, "On the number of modes in spherical wave expansions," in Proceedings of 26th AMTA, Stone Mountain Park, GA, USA, Oct. 17–22, 489–494 (2004).
26. J. Rubio, M. A. González, and J. Zapata, "Analysis of cavity-backed microstrip antennas by a 3-D finite element/segmentation method and a matrix Lanczos-Padé algorithm (SFELP)," IEEE Antennas Wirel. Propag. Lett. 1, 193-195 (2002), https://doi.org/10.1109/LAWP.2002.807783.
27. "How to measure errors."

https://www.netlib.org/lapack/lug/node75.html (accessed February 10, 2024).
28. C. S. Technology and Dassault Systèmes Vèlizy-Villacoublay France (2010), CST Studio Suite 2020, [Online]. Available: https://www.3ds.com/es/productos-y-servicios/simulia/productos/cst-studio-suite/

Table 1. Comparison of the matrix-to-invert sizes for two disks with radii equal to a wavelength

Separation between disks	Matrix size in this work	Matrix size in [21]
0.5λ	880	2176
0.2λ	880	5200

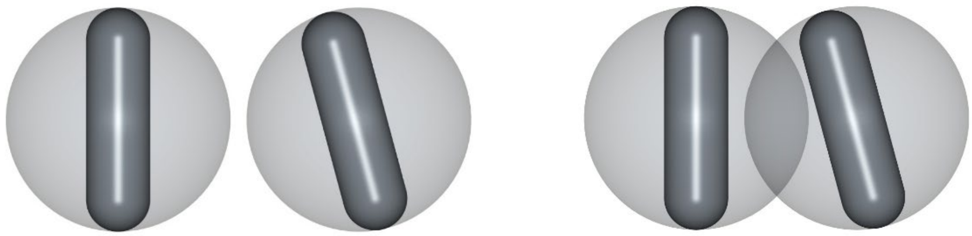

a) b)

Fig. 1

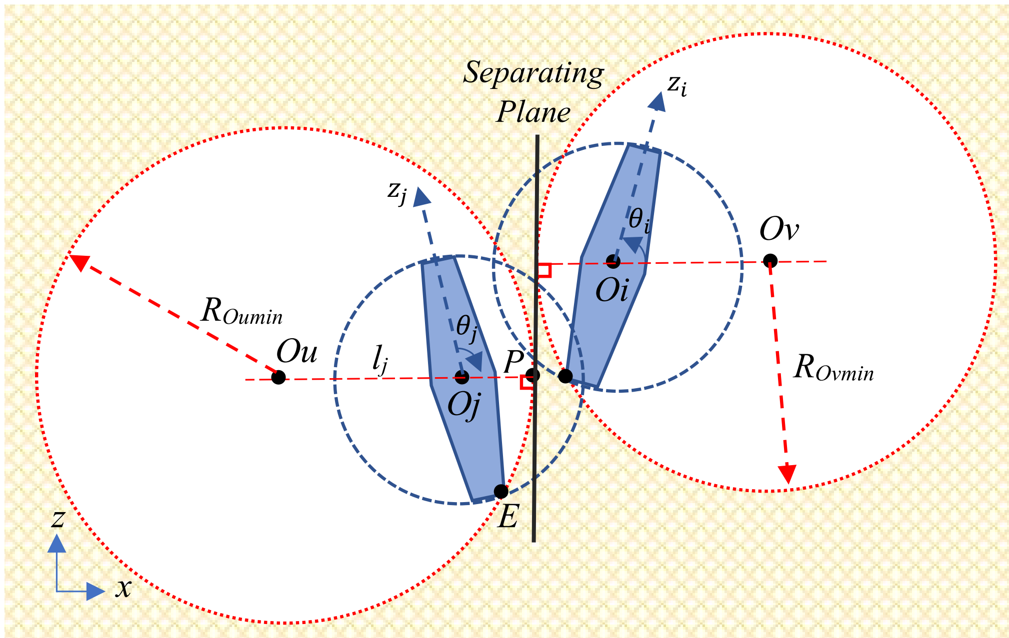

Separating
Plane
z_i
z_j
θ_i
Ov
R_{Oumin}
Oi
θ_j
Ou
l_j
P
R_{Ovmin}
Oj
E
z
x

Fig. 2

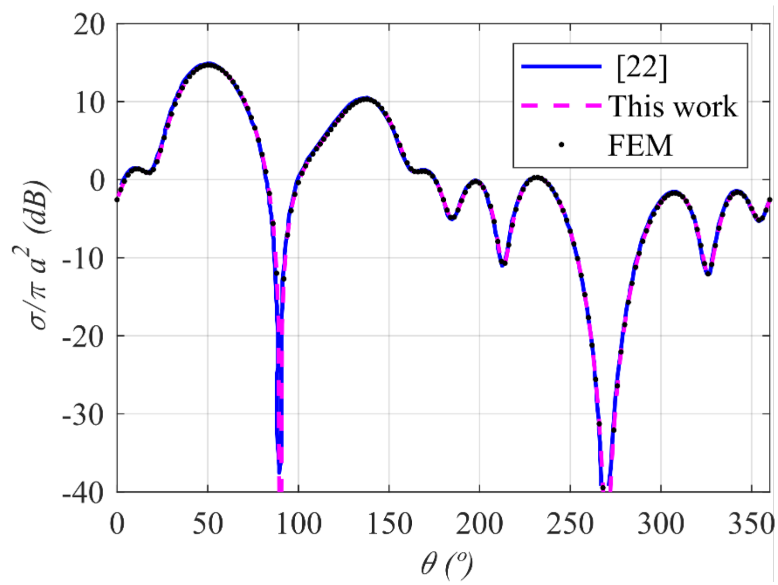
[22]
This work
FEM
σ/π a² (dB)
θ (°)
20
10
0
-10
-20
-30
-40
0
50
100
150
200
250
300
350

Fig.3

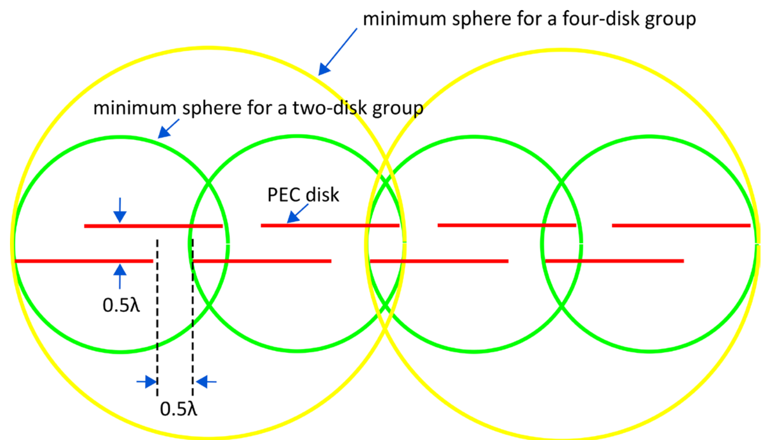
minimum sphere for a four-disk group
minimum sphere for a two-disk group
PEC disk
0.5λ
0.5λ

Fig. 4

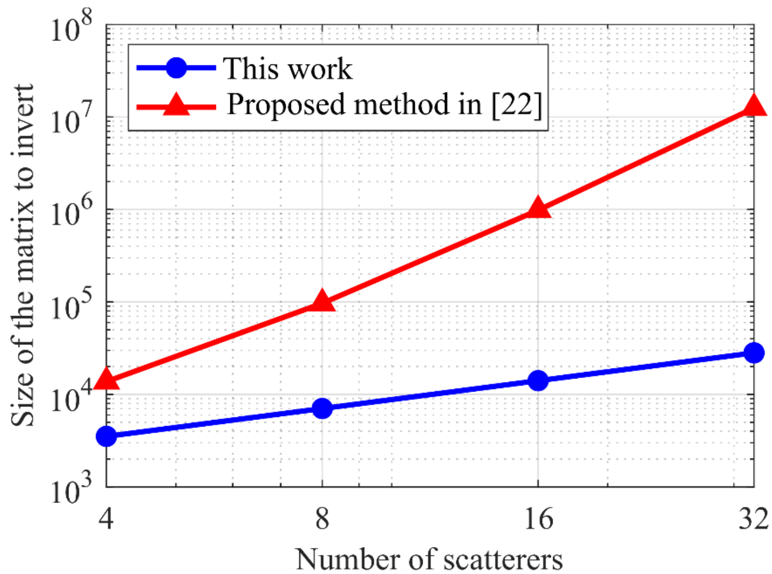

This work
Proposed method in [22]
Size of the matrix to invert
Number of scatterers

Fig. 5

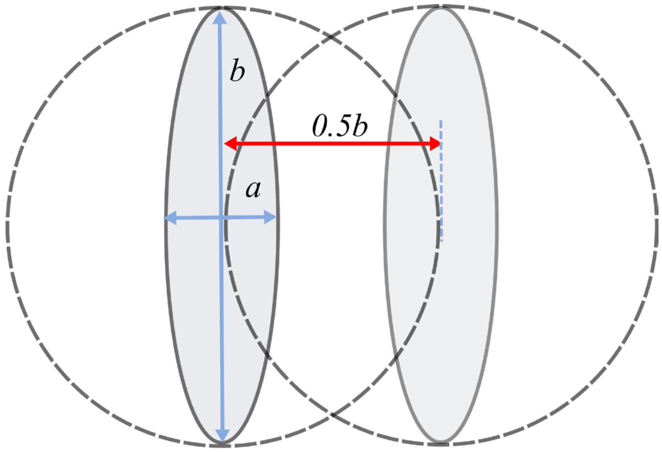

a)

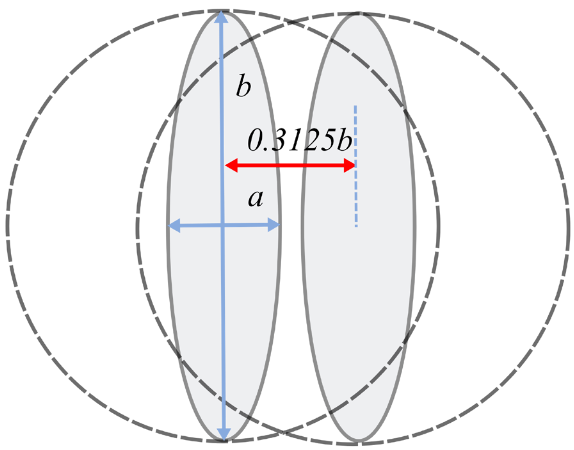

b)

Fig. 6

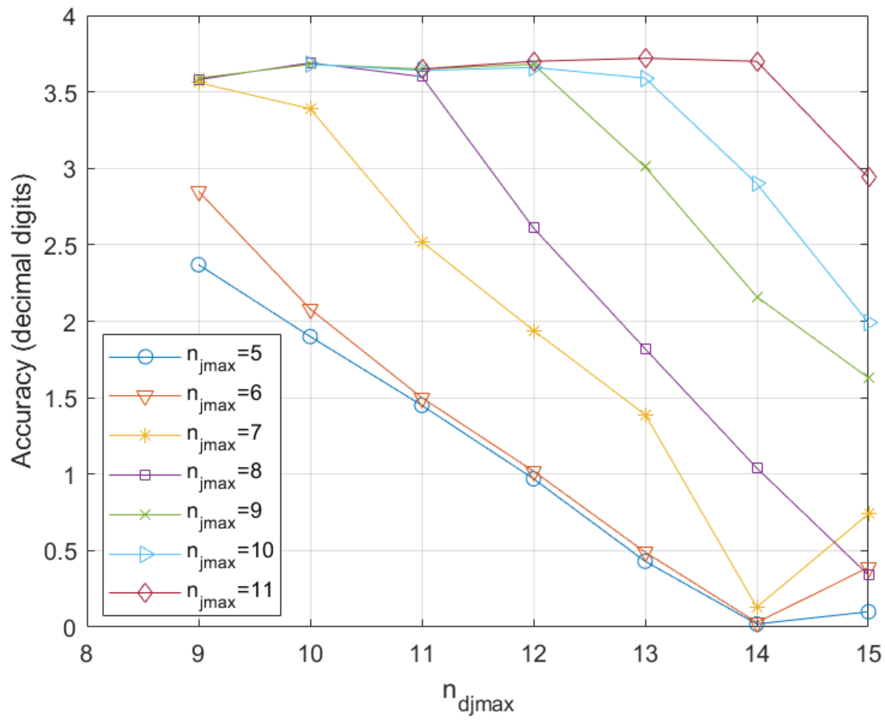

Accuracy (decimal digits)
n_{djmax}
n_{jmax}=5
n_{jmax}=6
n_{jmax}=7
n_{jmax}=8
n_{jmax}=9
n_{jmax}=10
n_{jmax}=11
0
0.5
1
1.5
2
2.5
3
3.5
4
8
9
10
11
12
13
14
15

Fig. 7

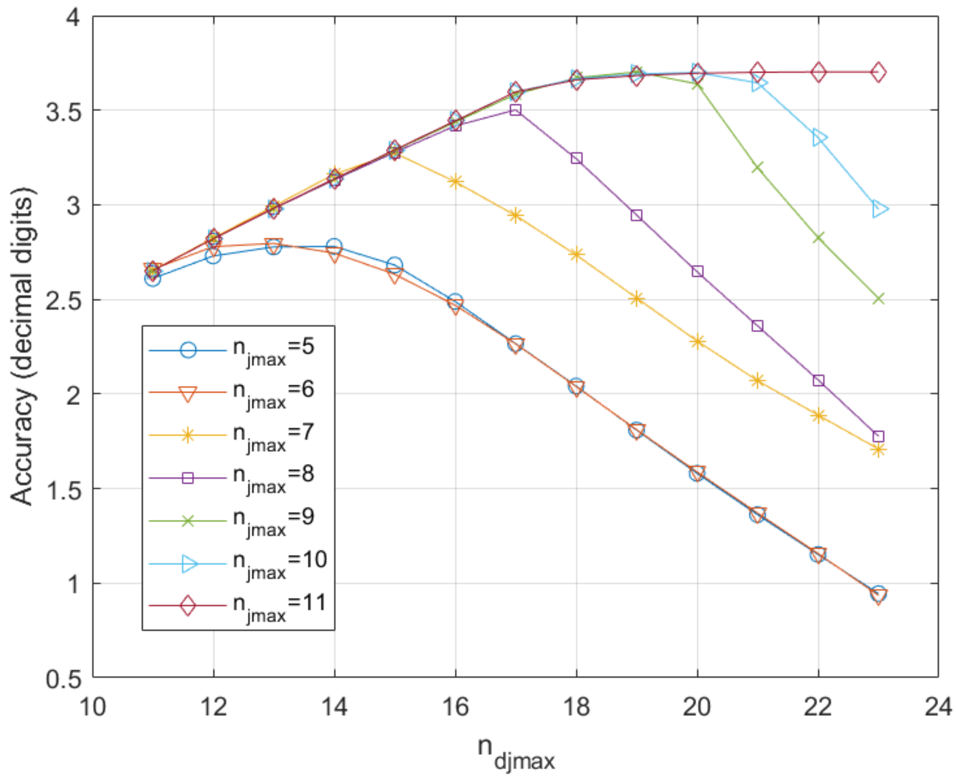

Accuracy (decimal digits)
n_{djmax}
n_{jmax}=5
n_{jmax}=6
n_{jmax}=7
n_{jmax}=8
n_{jmax}=9
n_{jmax}=10
n_{jmax}=11
4
3.5
3
2.5
2
1.5
1
0.5
10
12
14
16
18
20
22
24

Fig. 8

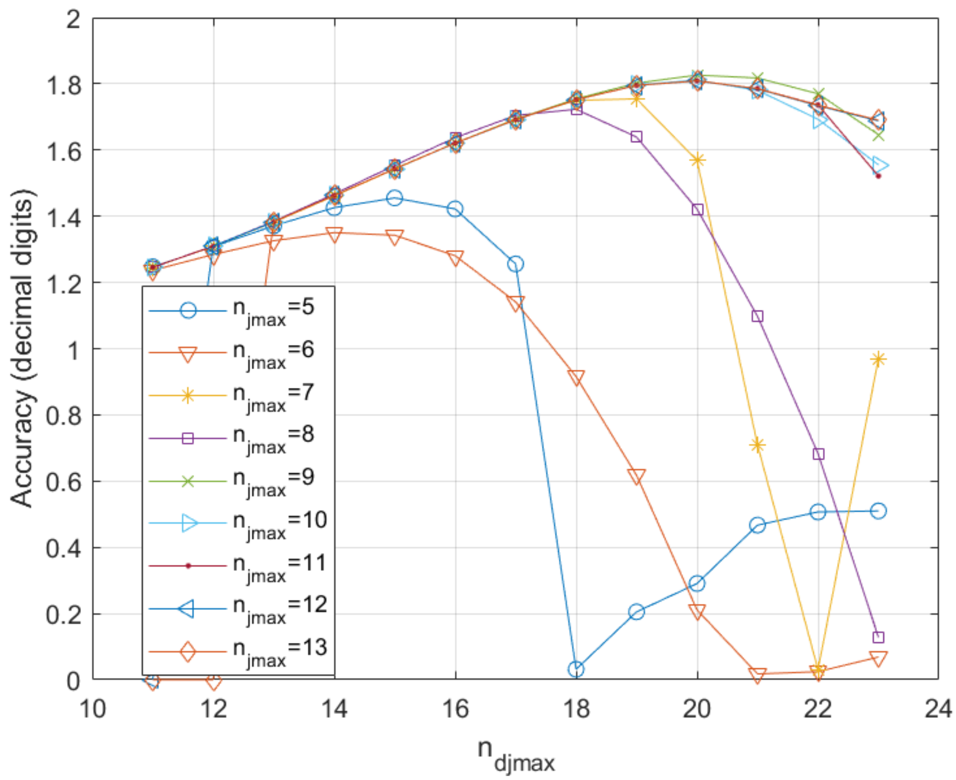

Accuracy (decimal digits)
n_{djmax}
n_{jmax}=5
n_{jmax}=6
n_{jmax}=7
n_{jmax}=8
n_{jmax}=9
n_{jmax}=10
n_{jmax}=11
n_{jmax}=12
n_{jmax}=13
0
0.2
0.4
0.6
0.8
1
1.2
1.4
1.6
1.8
2
10
12
14
16
18
20
22
24

Fig. 9

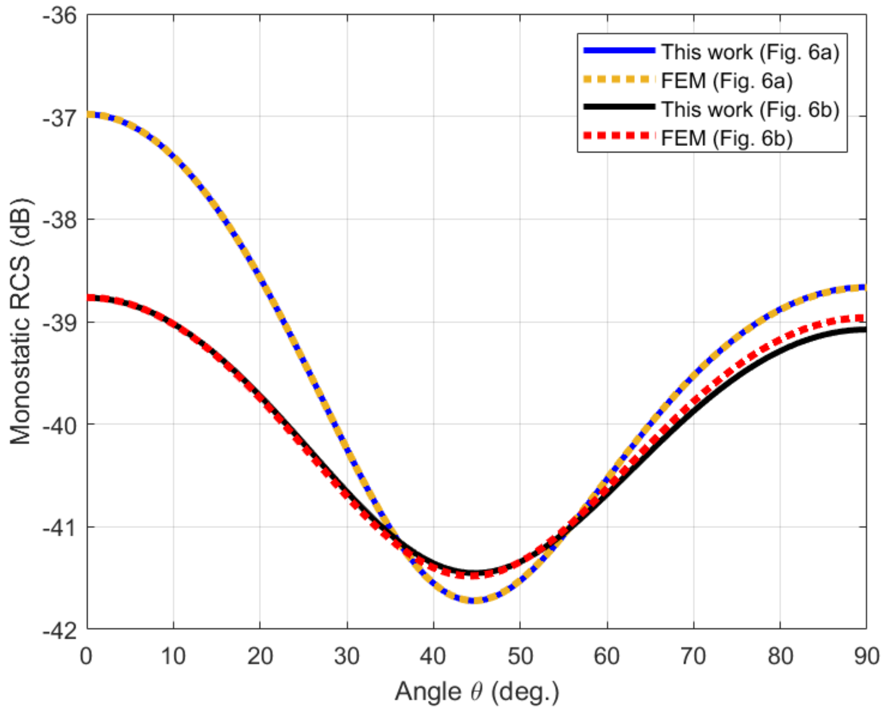

-36
-37
-38
-39
-40
-41
-42
Monostatic RCS (dB)
0
10
20
30
40
50
60
70
80
90
Angle θ (deg.)
This work (Fig. 6a)
FEM (Fig. 6a)
This work (Fig. 6b)
FEM (Fig. 6b)

Fig. 10

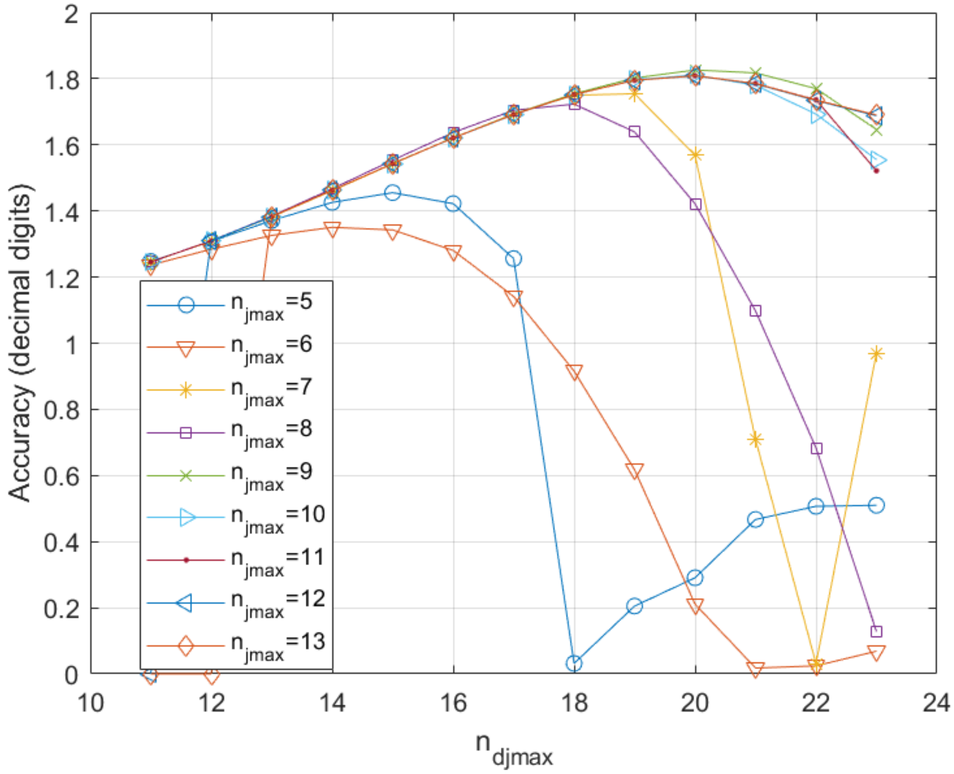

2
1.8
1.6
1.4
1.2
1
0.8
0.6
0.4
0.2
0
Accuracy (decimal digits)
10
12
14
16
18
20
22
24
n djmax
n jmax =5
n jmax =6
n jmax =7
n jmax =8
n jmax =9
n jmax =10
n jmax =11
n jmax =12
n jmax =13

Fig. 11

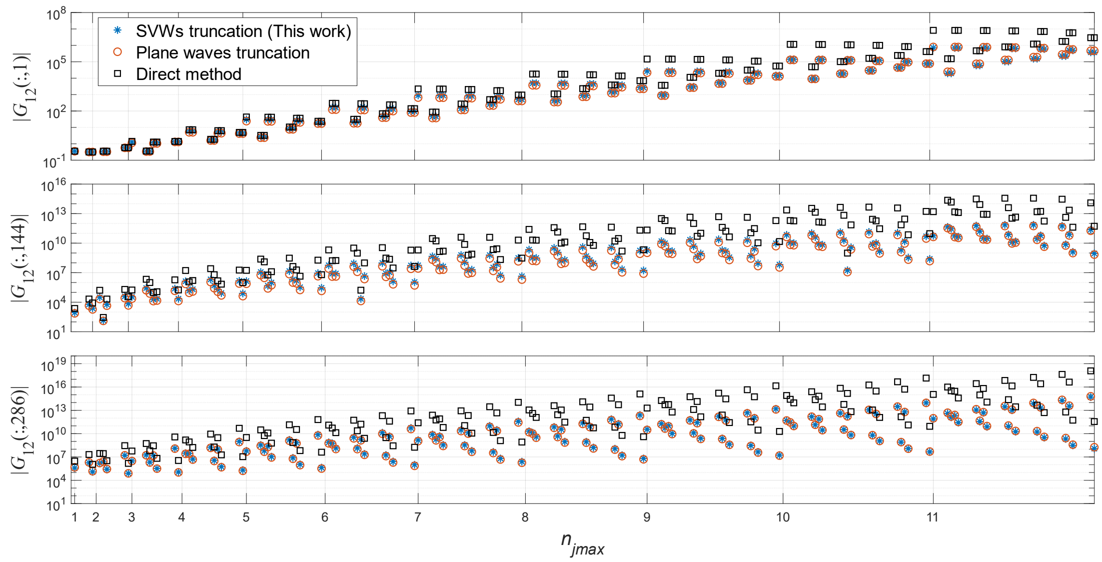
SVWs truncation (This work)
Plane waves truncation
Direct method
$|G_{12}(:,1)|$
$|G_{12}(:,144)|$
$|G_{12}(:,286)|$
n_{jmax}

Fig. 12

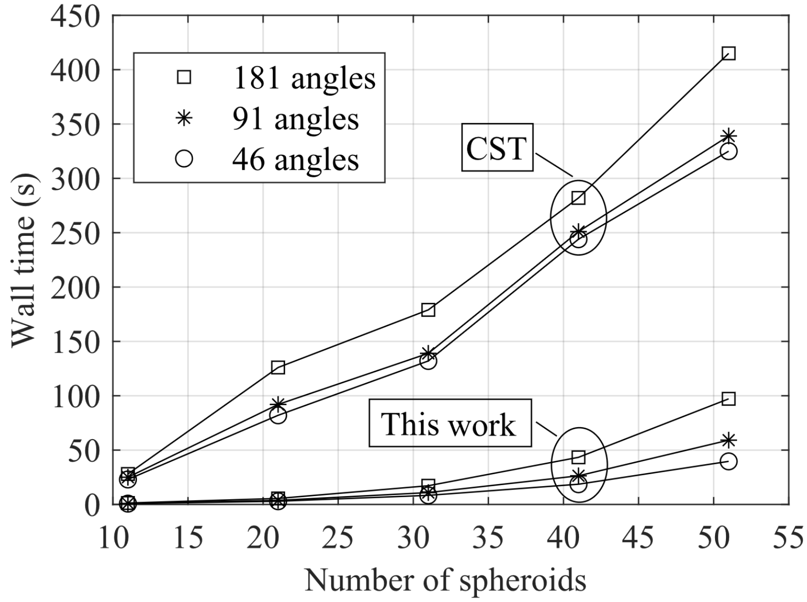
181 angles
91 angles
46 angles
CST
This work
Wall time (s)
Number of spheroids
0
50
100
150
200
250
300
350
400
450
10
15
20
25
30
35
40
45
50
55

Fig. 13

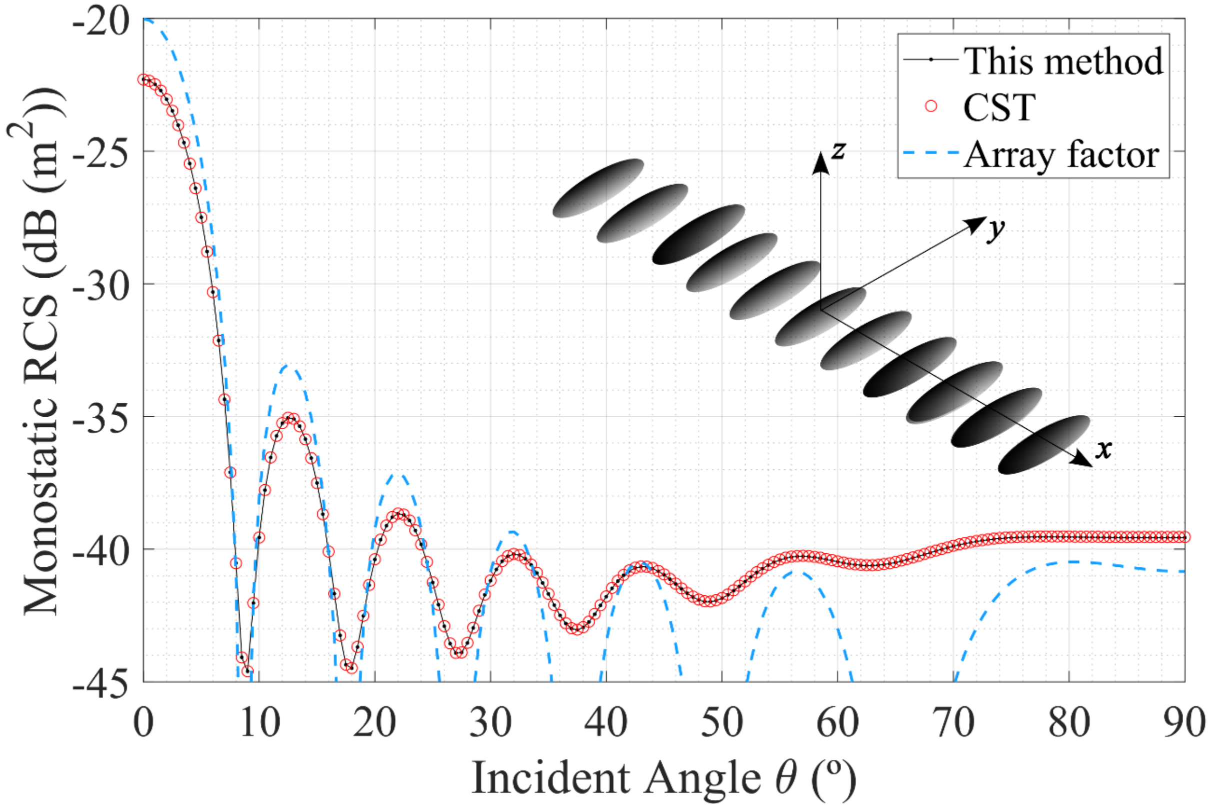

-20
-25
-30
-35
-40
-45
0
10
20
30
40
50
60
70
80
90
Monostatic RCS (dB (m^2))
Incident Angle θ (º)
This method
CST
Array factor
z
y
x

Fig. 14

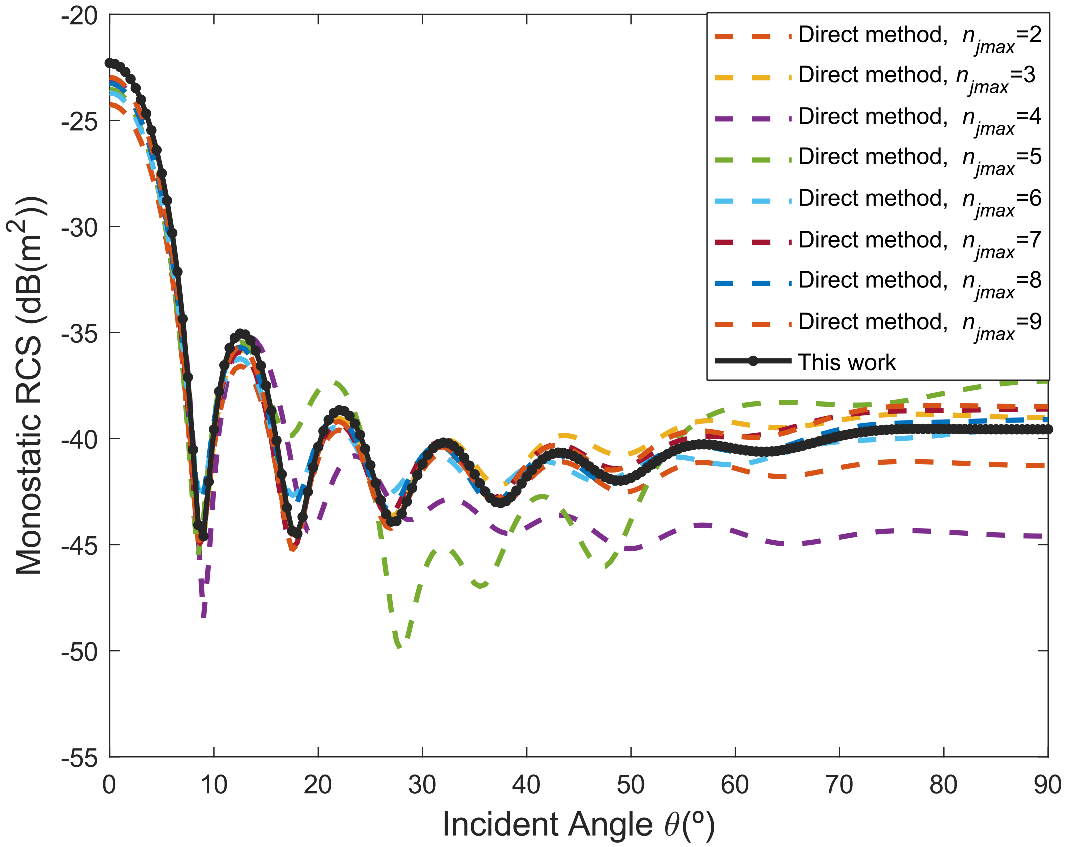

Direct method, n_{jmax}=2
Direct method, n_{jmax}=3
Direct method, n_{jmax}=4
Direct method, n_{jmax}=5
Direct method, n_{jmax}=6
Direct method, n_{jmax}=7
Direct method, n_{jmax}=8
Direct method, n_{jmax}=9
This work
Monostatic RCS (dB(m^2))
Incident Angle θ(º)
-20
-25
-30
-35
-40
-45
-50
-55
0
10
20
30
40
50
60
70
80
90

Fig. 15

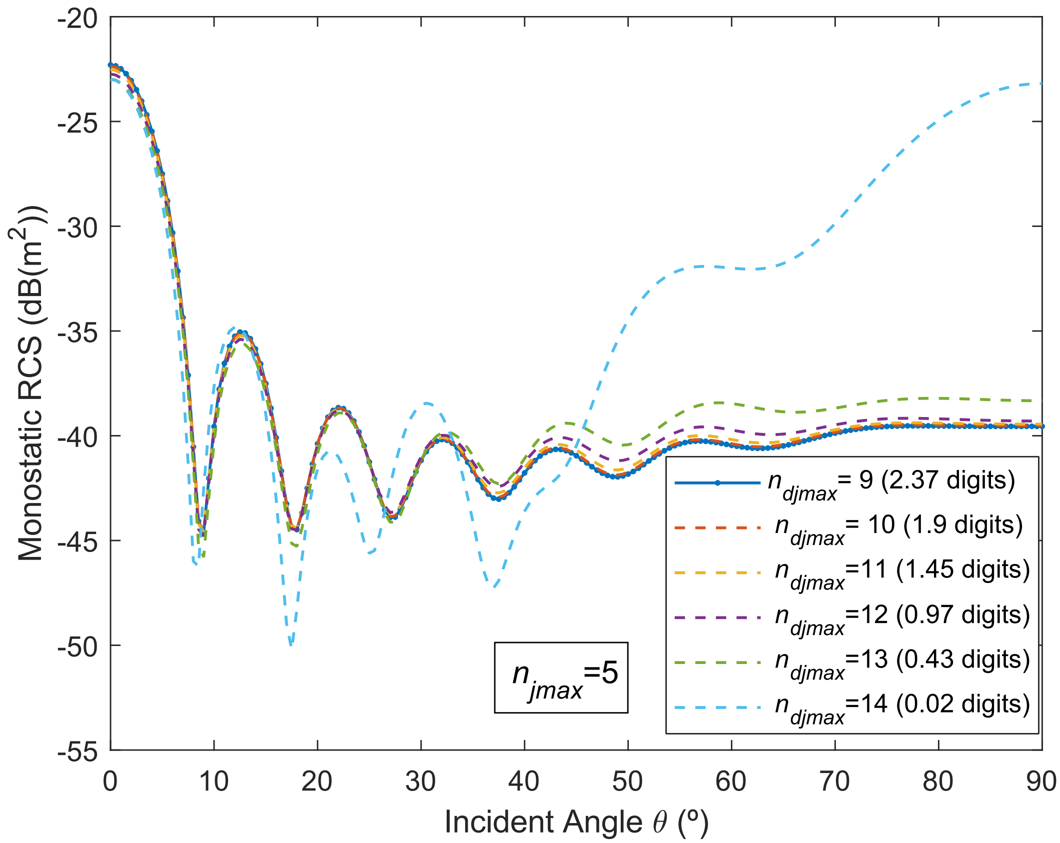

-20
-25
-30
-35
-40
-45
-50
-55
Monostatic RCS (dB(m^2))
0
10
20
30
40
50
60
70
80
90
Incident Angle θ (º)
n_{djmax}= 9 (2.37 digits)
n_{djmax}= 10 (1.9 digits)
n_{djmax}=11 (1.45 digits)
n_{djmax}=12 (0.97 digits)
n_{djmax}=13 (0.43 digits)
n_{djmax}=14 (0.02 digits)
n_{jmax}=5

Fig. 16

Fig 1. Minimum-circumscribing spheres for two particles in two scenarios: a) without overlap, b) with overlap.

Fig 2. 2-D representation of two particles centered in Oi and Oj, with overlapping minimum spheres, and a separating plane. From this plane two new centers for the particles, Ou and Ov, are obtained so that their minimum spheres do not overlap.

Fig. 3. Normalized bistatic radar cross section for two PEC disks with radius $a = \lambda$ separated a distance $d = 0.5\lambda$. Incident angle equal to 60º.

Fig. 4. Eight disks with radii equal to a wavelength and mutually overlapping minimum spheres.

Fig. 5. Maximum size of the matrices to invert as a function of the number of disks for the case depicted in Fig. 3.

Fig. 6. Two spheroids and their minimum spheres with a separation equal to: a) $0.5b$, b) $0.3125b$.

Fig. 7. Accuracy in terms of approximate number of decimal digits for different values of the maximum index n_{jmax} in its original coordinate system, as a function of the maximum index in the new center $n_{\mathrm{d}jmax}$, for the case depicted in Fig. 6a. Eq. (17) is computed with a distance of 0.78λ between the new centers.

Fig. 8. Accuracy in terms of approximate number of decimal digits for different values of the maximum index n_{jmax} in its original coordinate system, as a function of the maximum index in the new center $n_{\mathrm{d}jmax}$, for the case depicted in Fig. 6a. Eq. (17) is computed with a distance of 1.5λ between the new centers.

Fig. 9. Accuracy in terms of approximate number of decimal digits for different values of the maximum index n_{jmax} in its original coordinate system, as a function of the maximum index in the new center $n_{\mathrm{d}jmax}$, for the case depicted in Fig. 6b.

Fig. 10. Monostatic RCS calculated for two spheroids in Figs 6a and 6b at φ=0º. For every incident angle, a horizontally polarized field (parallel to the xy plane) was considered.

Fig. 11. Accuracy in terms of approximate number of decimal digits for different values of the maximum index n_{jmax} in its original coordinate system, as a function of the integral truncated value κ_{tr} normalized to the wavenumber k as defined in [14], for the case depicted in Fig. 6a.

Fig. 12. Coefficients of three columns of the general translation matrix for the case depicted in Fig. 6a. Comparison between this work ($n_{djmax} = 22$), the method based on plane waves transformation ($\kappa_{tr} = 3.75k$) and the direct method.

Fig. 13. Computing time for several spheroid groups, arranged in *x* axis as shown in the inset of Fig. 13. Several number of incident angles between θ=0º and θ=90º where analyzed.

Fig. 14. Monostatic RCS calculated for the group of 11 spheroids shown in the inset at ϕ=0º. For every incident angle, a horizontally polarized field (parallel to the *xy* plane) was considered.

Fig. 15. Convergence analysis of the proposed method compared with the direct method. Same case as in Fig. 13, but with several values of n_{jmax}. Results do not converge and for $n_{jmax} =$

9 a matrix close to singular is obtained. Our approach (labeled as “This work”) does not suffer that lack of convergence as all the results are indistinguishable for $n_{djmax} = 9$ and n_{jmax} from 5 to 9.

Fig. 16. Convergence analysis of the proposed method for $n_{jmax} = 5$. Same case as in Fig. 13, but with several values of n_{djmax}. It has been included the number of digits of accuracy of the 2-spheroid case for each value of n_{djmax} obtained in Fig. 7.